

14,04

## Nanocomposites based on thermoplastic aromatic polyimides with cerium dioxide nanoparticles: dielectric spectroscopy

© N.A. Nikonorova<sup>1</sup>, A.A. Kononov<sup>2</sup>, R.A. Kastro<sup>2</sup>, I.V. Gofman<sup>1</sup>, A.L. Nikolaeva<sup>1</sup>,  
I.V. Abalov<sup>1</sup>, A.V. Yakimansky<sup>1</sup>, A.E. Baranchikov<sup>3</sup>, V.K. Ivanov<sup>3</sup>

<sup>1</sup> Institute of Macromolecular Compounds, Russian Academy of Sciences,  
St. Petersburg, Russia

<sup>2</sup> Herzen State Pedagogical University of Russia,  
St. Petersburg, Russia

<sup>3</sup> Institute of General and Inorganic Chemistry, Russian Academy of Sciences,  
Moscow, Russia

E-mail: n\_nikonorova2004@mail.ru

Received April 5, 2022

Revised April 5, 2022

Accepted April 11, 2022

The molecular mobility of films of thermoplastic aromatic polyimides and nanocomposites based on them with 3% cerium dioxide has been studied by dielectric spectroscopy. Three relaxation regions of dipole polarization were found for the initial polyimides,  $\gamma$  and  $\beta$  (in the glassy state) and  $\alpha$  (transition to a highly elastic state). The introduction of 3% cerium dioxide into the matrix polyimide leads to the suppression of the  $\gamma$  process and to the appearance in the spectra of nanocomposites, along with the  $\beta$  process, of the second relaxation process  $\beta_1$ . The temperature dependences of the relaxation time for the  $\gamma$ ,  $\beta$  and  $\beta_1$  processes are linear and correspond to the Arrhenius equation, and for the  $\alpha$  process are curved and described by the Vogel–Tamman–Hesse equation. The interpretation of the molecular mechanisms of the observed processes is given.

**Keywords:** Polymer-inorganic nanocomposites, aromatic polyimides, nanoscale cerium dioxide, dielectric characteristics, transition temperatures, molecular mechanisms of dielectric processes.

DOI: 10.21883/PSS.2022.08.54636.333

### 1. Introduction

Thermoplastic aromatic polyimides (PI) [1,2], which differ by a large variety of chemical structure and, accordingly, physical properties, are widely used in microelectronics, electrical engineering, which is caused by their unique electric characteristics (specific resistance  $\rho_v \sim 10^{15} \Omega/\text{m}$  and relatively low dielectric permeability  $\epsilon \sim 2.5\text{--}3.5$ ). One of the methods to optimize a complex of polymer material properties, widely used in current papers, is production of composites by addition of various fillers into a polymer matrix. Recently composites based on thermoplastic PIs and nanoscale particles of most diverse nature and geometry such as nanotubes, fullerenes, graphenes etc. are of great interest. Interactions between nanoparticles and macromolecules of the polymer matrix cause change in properties of the original polymer material [3–8]. Research of mechanisms used by nanoparticles to impact composite properties are of great interest, as well as prediction of properties depending on the type and structure of nanoparticles and their concentration.

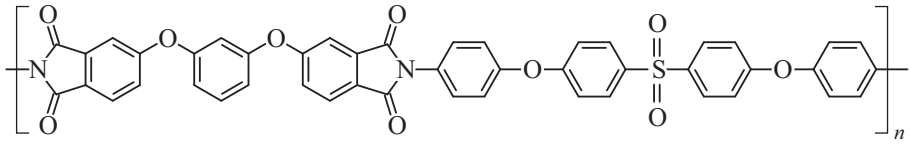
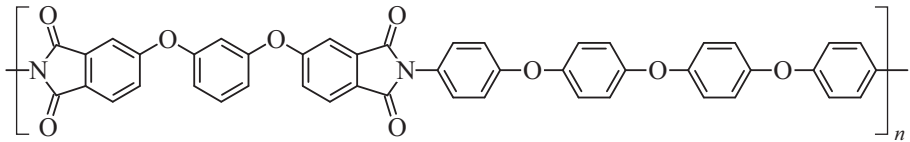
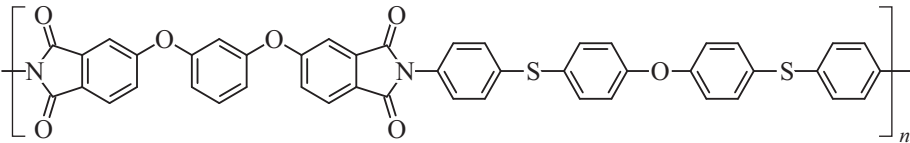
Papers published in the recent years present results of research of thermoplastic aromatic polyimides and nanocomposites on their basis using various experimental methods (mechanical tests, DSC, thermogravimetry, X-ray diffraction analysis, dielectric methods etc.), each providing information about specific properties of these materials [9–13].

Valuable information about the considered issues may be obtained by the method of dielectric spectroscopy (DS). This is one of the modern physical methods of research making it possible to study processes related to molecular mobility in a polymer sample placed in the external AC electric field with frequency  $\omega$ . Such research is a critical tool to collect data on molecular mobility of various kinetic units (individual atoms, groups, segments), which carry a polar group, in the wide range of temperatures and frequencies. Interpretation of dielectric spectrum is based on comparison of dielectric behavior of systems similar in chemical composition [11,14–20]. This makes it possible to identify observed relaxation processes and relate them to mobility of certain kinetic units, which include a polar group.

Besides, DS is a convenient and fast method to measure electric conductivity of the material, which is important when PIs are used in microelectronics.

Among a wide selection of various nanoparticles used to form PI-based nanocomposites, nanoscale cerium oxide — nanoparticles with size of  $\sim$  units of nanometers have been of great interest, as confirmed by results obtained in new papers [21–23]. Their introduction into PI films makes it possible to modify various groups of material properties, in particular, mechanical characteristics and material heat resistance. With account of previously obtained results, it seemed feasible to study the impact of this nanoscale

**Table 1.** Structures and designations of PIs used in the work

№	Equation	Designation
1		P-SOD
2		P-OOD
3		P-SOS

filler at characteristics of thermally stimulated physical transitions implemented in thermoplastic PIs, at molecular mobility implemented in these materials in a wide range of frequencies and temperatures. Detailed study of these features in behavior of nanocomposite films „PI-CeO<sub>2</sub>“, formed on the basis of some thermoplastic polynuclear PIs, which differ by structure of diamine part of an elementary unit, was the objective of this paper.

## 2. Experimental part

As matrix PIs, based on which nanocomposite films were formed, and as reference polymer samples, three thermoplastic polynuclear PIs were used, whose structures are given in Table 1.

Nanocomposite films containing 3 mass.% CeO<sub>2</sub>, as reference samples of PIs, with thickness of 25–40 μm, were prepared using a method of double-stage synthesis [1–2]. Polyamidoacids (PAA) — prepolymers of corresponding PIs as solutions in N-methylpyrrolidone were obtained in the Institute of Macromolecular Compounds, Russian Academy of Sciences, according to method [24].

Quasispherical nanoparticles of cerium oxide with size of 5–6 nm are synthesized in the Institute of General and Inorganic Chemistry of the Russian Academy of Sciences. The synthesis protocol is described in detail in [25].

To form nanocomposites, the rated quantities of nanoparticles were dispersed in N-methylpyrrolidone using an ultrasonic disperser, and then the produced homogeneous dispersion was introduced in the rated quantity of PAA solution with subsequent homogenization of the solution using an overhead drive mechanical mixer. Using the produced nanocomposite solutions, as well as solutions of reference PAAs, films were prepared with compositions „PAK-CeO<sub>2</sub>“ and source PAAs, accordingly, by pouring

onto glass substrates. Then films were dried (80°C — 4 h), and their thermal cyclization was carried out (heating to 300°C with delay at this temperature for 0.5 h).

Thermomechanical analysis of films was carried out using analyzer TMA 402 F1 Hyperion (Netzsch, Germany) in the sample heating mode from –100°C to change to devitrified state with speed 5 deg·min<sup>–1</sup> when the sample is exposed to dynamic stretching force with frequency 1 Hz and amplitude 1 MPa on the background of permanent stretching tension 2 MPa.

Dielectric spectra of PI and nanocomposite films were produced using broadband dielectric spectrometers „Concept-22“ and „Concept-81“ by „Novocontrol Technologies“ with an automatic frequency analyzer of high resolution ALPHA-ANB. Samples were films pressed between brass electrodes (diameter of the upper electrode 20 mm) at temperature that is ~ 30°C higher than vitrification temperature (the values of the latter were first determined by thermomechanical method). Dielectric measurements were carried out in the range of frequencies 0.1–3 · 10<sup>6</sup> Hz and temperatures –100 – +390°C.

To obtain quantitative characteristics of observed relaxation processes, the complex dielectric permeability  $\varepsilon^* = \varepsilon'(\omega) - i\varepsilon''(\omega)$  was described by empirical equation of Havriliak — Negami (HN) [26]:

$$\varepsilon^*(\omega) - \varepsilon_\infty = \sum_{k=1}^n \text{Im} \left[ \frac{\Delta\varepsilon_k}{\{1 + (i\omega\tau_{HNk})^{\alpha_k}\}^{\beta_k}} \right], \quad (1)$$

where  $\Delta\varepsilon$  — increment of dielectric permeability;  $\Delta\varepsilon = \varepsilon_0 - \varepsilon_\infty$ ,  $\varepsilon_0 = \varepsilon'$  at frequency  $\omega \rightarrow 0$ ,  $\varepsilon_\infty = \varepsilon'$  at  $\omega \rightarrow \infty$ ;  $\tau_{HN}$  — characteristic time of Havriliak–Negami relaxation;  $\alpha_{HN}$  and  $\beta_{HN}$  — parameters compliant with expansion and asymmetry of relaxation time distribution, accordingly;  $k$  — number of relaxation processes.

The most probable relaxation time  $\tau_{\max}$ , compliant with the relaxation time value at  $\epsilon''_{\max}$  on dependence  $\epsilon'' = \varphi(\omega)$ , is defined as [27]:

$$\tau_{\max} = \tau_{HN} \left[ \frac{\sin\left(\frac{\pi(\alpha_{HN})\beta_{HN}}{2(\beta_{HN}+1)}\right)}{\sin\left(\frac{\pi(\alpha_{HN})}{2\beta_{HN}+1}\right)} \right]^{1/\alpha_{HN}} \quad (2)$$

Separation of processes and calculation of their parameters was carried out using software WinFit „Novocontrol Technologies“, based on minimization of the sum of squared deviations of functions from the sought variables.

### 3. Results and discussion

As it was noted in the experimental part, production of quality samples for dielectric tests required pressing of investigated films between brass electrodes at temperatures exceeding vitrification temperatures  $T_g$  of the corresponding polymer materials by  $\sim 30^\circ\text{C}$ . To perform this preparatory operation, at the first stage of the work the values  $T_g$  of used polymers and composites were defined by thermomechanical method (Table 2).

The results produced make it possible to form an important conclusion about complete identity of vitrification temperatures of the film of each of used PIs and the nanocomposite film made on its basis.

When curves of temperature dependences of mechanical loss angle tangent is analyzed (example for film P-SOD — in Fig. 1), an additional transition is also identified in the area below  $T_g$ . For P-COD it is implemented at temperature  $86^\circ\text{C}$  (measurement at frequency 1 Hz, amplitude of oscillations of extending load 1 MPa).

Results from studies of various PIs by dielectric method that are characterized by a large variety of structures of both diamine and dianhydride components of the macromolecule elementary unit are given in papers [11,14–16,28–34]. As a rule, dielectric spectra (dependences  $\epsilon'' = \varphi(\omega)$ ) of these materials demonstrated availability of at least three maximum areas, provided for by dipole polarization relaxation processes, since maximum  $\epsilon''$  moved towards higher frequencies as temperature grew. These processes meant at temperature grew, as  $\gamma$  and  $\beta$  (in glassy state) and  $\alpha$  when changing to highly elastic state.

**Table 2.** Vitrification temperatures of researched PIs and composites with  $\text{CeO}_2$

№	Film composition	$T_g, ^\circ\text{C}$
1	P-SOD	217
2	P-SOD + $\text{CeO}_2$	216
3	P-OOD	179
4	P-OOD + $\text{CeO}_2$	179
5	P-SOS	185
6	P-SOS + $\text{CeO}_2$	183

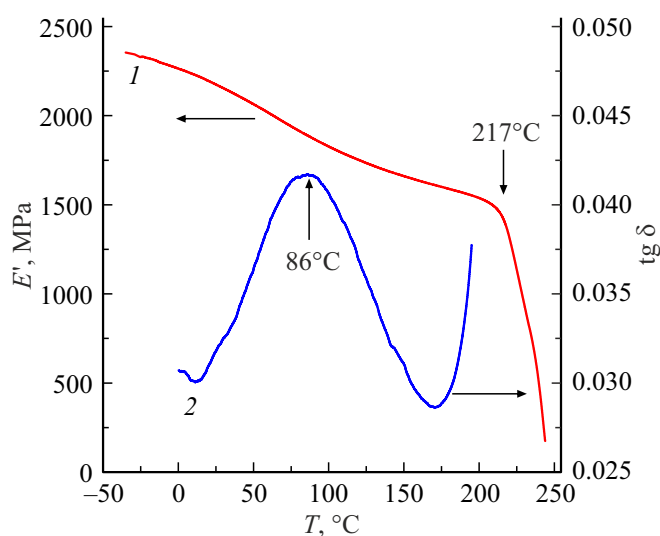


**Figure 1.** Thermomechanical curves of film P-SOD: temperature dependences of module  $E'$  and tangent of angle of mechanical losses.

To visualize dielectric behavior of studied samples in the entire temperature range, temperature dependences were built for tangent of dielectric losses angle  $\text{tg}\delta$  at various frequencies for films of nanocomposites and matrix polymers. As for the PIs studied before, for initial samples P-SOD, P-OOD and P-SOS three relaxation processes were observed,  $\gamma$ ,  $\beta$  and  $\alpha$ . For nanocomposites, only  $\alpha$  and  $\beta$  processes were observed. All three pairs of samples (PIs and nanocomposite on its basis) gave a similar picture of dielectric behavior. Fig. 2 shows, as an example, the temperature dependences  $\text{tg}\delta$  for films P-OOD (a) and composite P-OOD +3%  $\text{CeO}_2$  (b).

Comparison of dielectric behavior of film P-OOD and corresponding nanocomposite at frequency 1 kHz is demonstrated by Fig. 3.

It is seen that in area of  $\alpha$  transition the introduction of  $\text{CeO}_2$  practically does not change the position of maximum  $\text{tg}\delta$  and intensity of the process. It means that introduction of nanoparticles will not change the molecular mobility in the area of  $\alpha$ -process. This result is well compliant with data collected by thermomechanical method (Table 2). At the same time, in nanocomposites in glassy state (at temperatures below  $\alpha$  transition) compared to initial PIs, there is a significant growth of dielectric losses, as a result of which  $\gamma$  process may not be observed.

The most probable relaxation times for all observed relaxation processes, both for initial PIs and for nanocomposites, are calculated from frequency dependences  $\epsilon''$  by equations (1) and (2). As an example, frequency dependences were given  $\epsilon''$  for P-SOD in area  $\gamma$  and  $\beta$  processes (Fig. 4, a, 4, b, accordingly) and for P-SOS in the field  $\alpha$  of the process (Fig. 4, c), described by equation HN. For area of  $\alpha$  process, a contribution was also taken into account, provided for by conductivity:  $\frac{\sigma_{dc} \cdot d}{\epsilon_0 \cdot \omega^s}$ , where

**Table 3.** Parameters of equation (3):  $-\lg \tau_0$ , and  $E_a$ , describing  $\gamma$ ,  $\beta_1$  and  $\beta$  processes for films of studied PIs and nanocomposites

Sample	$-\lg(\tau_0, s)$	$E_a, \text{kcal/mol}$	$-\lg(\tau_0, s)$	$E_a, \text{kcal/mol}$	$-\lg(\tau_0, s)$	$E_a, \text{kcal/mo}$
	$\gamma$ -process		$\beta_1$ -process		$\beta$ -process	
P-SOD	14.5	9.9			20.3	32
P-SOD 3% CeO <sub>2</sub>			12.5	14.8	19.17	27.2
P-SOS	14.1	10.1			19.4	28.5
P-SOS 3% CeO <sub>2</sub>			14.3	15.0	21.4	30.5
P-OOD	14.72	10.3			20.1	28.4
P-OOD 3% CeO <sub>2</sub>			14.2	15.2	20.3	28.2

$\sigma_{dc}$  — specific conductivity for DC,  $s$  and  $a$  — estimated parameters:  $s = 1$  (in case of ohmic conduction) or less than 1 (in all other cases),  $\epsilon_v = 8.854 \text{ pF/m}$  — dielectric permeability of vacuum.

For all initial PIs areas  $\gamma$  and  $\beta$  of dipole polarization relaxation are reliably described by one HN process (Fig. 4, *a* and 4, *b*, accordingly). In area of  $\alpha$  process, both for PIs

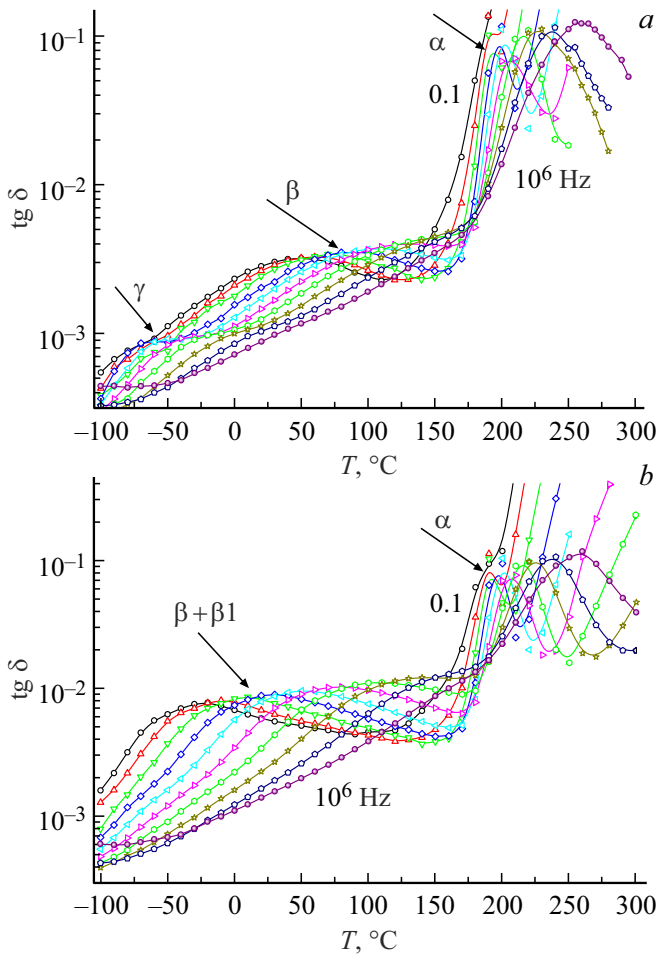


**Figure 2.** Temperature dependences  $\text{tg } \delta$  for P-OOD (*a*) and composite P-OOD + CeO<sub>2</sub> (*b*) at frequencies  $0.1 - 1 \cdot 10^6 \text{ Hz}$ . Frequency, at which each subsequent curve was obtained, is  $\sim 5$  times higher than the frequency of the previous curve.

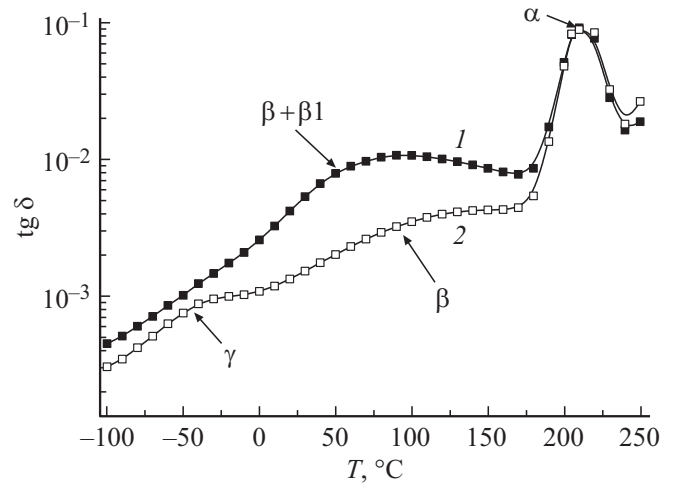


**Figure 3.** Temperature dependences  $\text{tg } \delta$  for P-OOD (*1*) and P-OOD + 3% CeO<sub>2</sub> (*2*) at frequency 1 kHz.

and for nanocomposite, dielectric spectra are described by one HN process with account of conductivity contribution (Fig. 4, *c*).

Dielectric behavior of nanocomposites in glassy state is characterized by two features compared to PI behavior. First, it was not possible to identify  $\gamma$  process, which is due to higher intensity of dielectric losses in this area of temperatures (Fig. 3). Second, for all three nanocomposite films  $\beta$ -relaxation may not be described by one HN process, and only by sum of two HN processes (Fig. 5).

For all studied systems, relaxation times,  $\tau_{\text{max}}$ , were calculated according to equations (1) and (2). As an example of dependence  $-\lg \tau_{\text{max}}$ , on reciprocal temperature for P-OOD (*a*) and P-OOD + 3% CeO<sub>2</sub> (*b*) are given in Fig. 6.

For  $\gamma$ ,  $\beta$  and  $\beta_1$  processes of dependence  $-\lg \tau_{\text{max}}$ , on reciprocal temperature are linear, and described by Arrhenius equation (Fig. 6, curves *1, 2, 4*):

$$\tau(T)_{\text{max}} = \tau_0 \exp\left(\frac{E_a}{RT}\right), \quad (3)$$

where  $\tau_0 = \tau_{\text{max}}$  at  $T \rightarrow \infty$ ,  $E_a$  — energy of activation of the relaxation process,  $R$  — universal gas constant.

Linear dependence  $-\lg \tau_{\max} = \varphi(1/T)$  is typical for local forms of molecular mobility described by Debye model, when the process of dipole reorientation is determined only

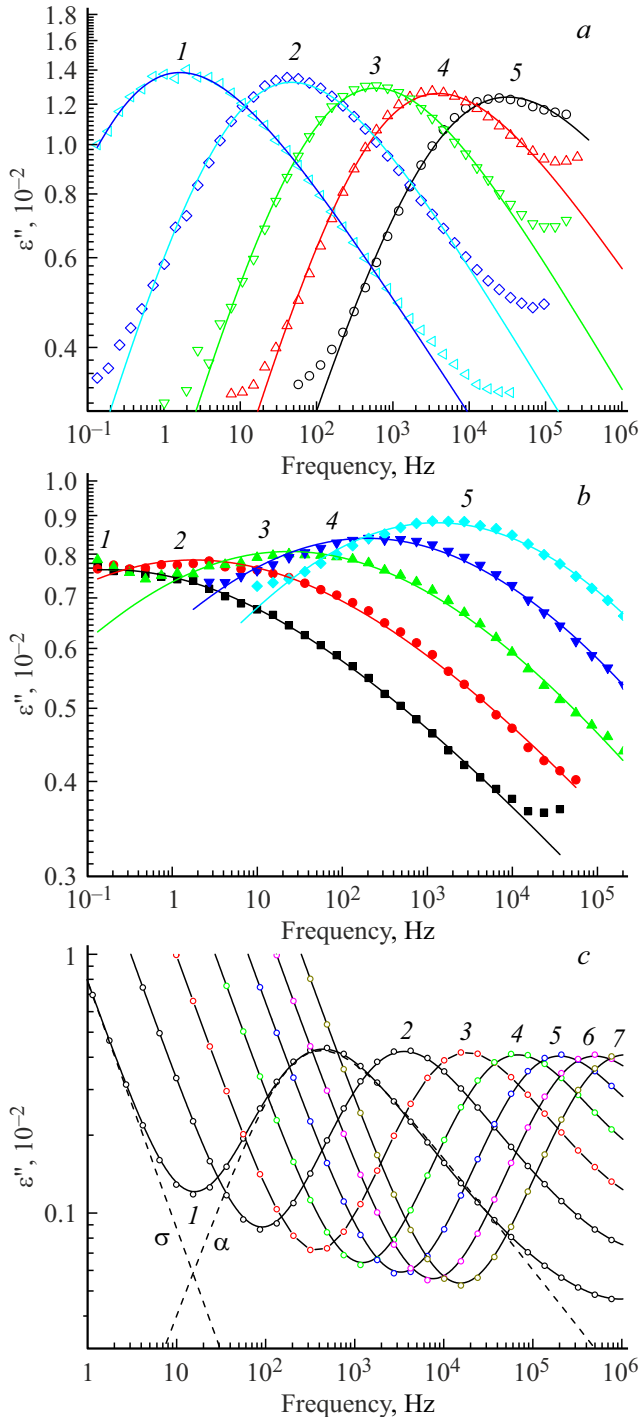


**Figure 4.** Frequency dependences  $\epsilon''$ , described by equation HN (solid lines), points of experimental data. (a) P-SOD — area of  $\gamma$  process at  $-100$  (1),  $-80$  (2),  $-60$  (3),  $-40$  (4) and  $-20^\circ\text{C}$  (5); (b) P-SOD — area of  $\beta$  process at  $60$  (1),  $80$  (2),  $100$  (3),  $120$  (4) and  $140^\circ\text{C}$  (5); (c) P-SOS — area of  $\alpha$  process at  $200$  (1),  $210$  (2),  $220$  (3),  $230$  (4),  $240$  (5),  $250$  (6) and  $260^\circ\text{C}$  (7); dashed lines — example of dielectric spectrum separation at  $200^\circ\text{C}$  into  $\alpha$  process and contribution due to conductivity  $\sigma$ .

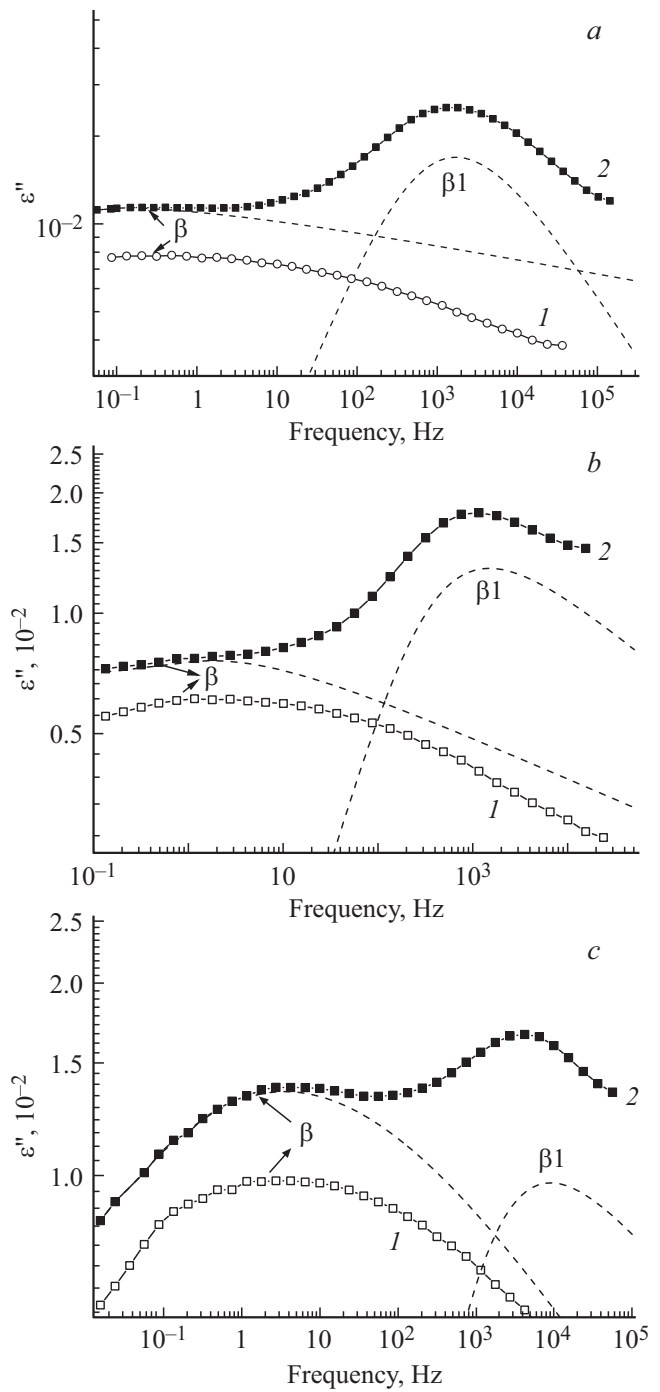


**Figure 5.** Frequency dependences  $\epsilon''$  at  $70^\circ\text{C}$ , described by one HN process for P-SOD (a), P-OOD (b) and P-SOS (c) and two HN processes for composites SOD + 3%  $\text{CeO}_2$  (a), P-OOD + 3%  $\text{CeO}_2$  (b) and P-SOS + 3%  $\text{CeO}_2$  (c); 1 and 2 — experimental data for PIs and nanocomposite, accordingly; dashed lines — separation of dielectric spectrum into  $\beta$  and  $\beta_1$  processes.

by intermolecular interactions and may be characterized in the entire range of temperatures by one value of activation energy [11,14–16]. Parameters of equation (3),  $-\lg \tau_0$ , and  $E_a$ , for  $\gamma$ ,  $\beta_1$  and  $\beta$  processes are given in Table 3.

For  $\alpha$  process the dependence  $-\lg \tau_{\max} = \varphi(1/T)$  is curvilinear (Fig. 6, curves 3) and is well described by empirical equation of Vogel–Tamman–Hesse (V–T–H) [35].

$$\tau_{\max} = \tau_0 \exp\left(\frac{B}{T - T_0}\right), \quad (4)$$

where  $\tau_0$ ,  $B$  and  $T_0$  — rated parameters that do not depend on the temperature ( $\tau_0$  — pre-exponential factor,  $B$  — activation parameter,  $T_0$  — so called Vogel temperature).

Non-linearity of dependences  $-\lg \tau_{\max} = \varphi(1/T)$  is specific for cooperative forms of molecular mobility, which includes, first of all,  $\alpha$  process, provided for by segmental mobility and related to transition to highly elastic state [31]. For the studied systems, dependences  $-\lg \tau_{\max} = \varphi(1/T)$  in the area of  $\alpha$  process are reliably described by equation 4). Values of parameters included in the equation are given in Table 4.

For initial PIs and nanocomposites the frequency dependences of the valid part of the complex specific conductivity,  $\sigma_{aac} = \varphi(f)$ , in the double logarithmic scale are qualitatively similar. As example, Fig. 7 gives dependences

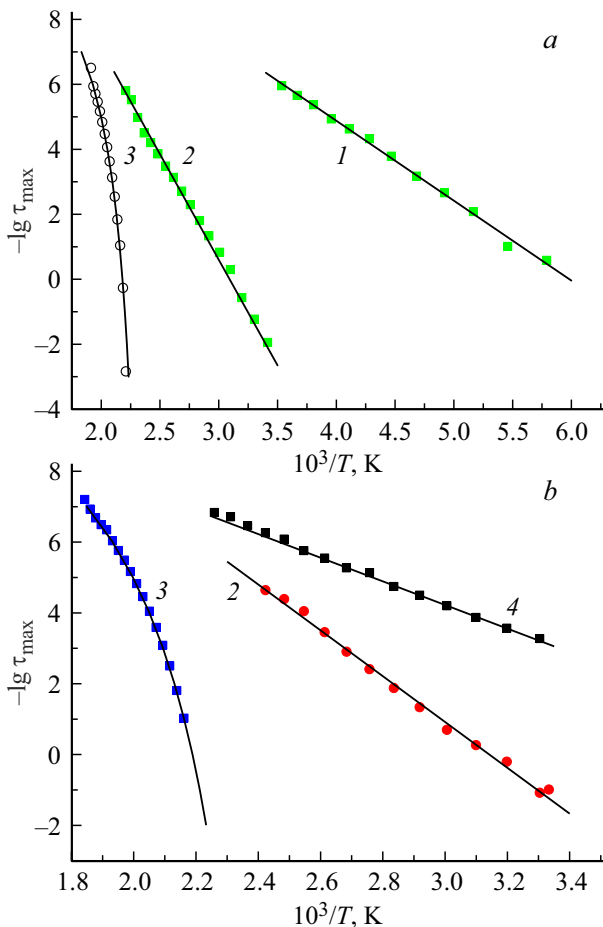


**Figure 6.** Dependences  $-\lg \tau_{\max}$  on reciprocal temperature for P-OOD (a) and P-OOD + 3% CeO<sub>2</sub> (b) for  $\gamma$  (1),  $\beta$  (2),  $\beta_1$  (4) and  $\alpha$  (3) processes. Points — calculations of  $\tau_{\max}$  according to equation HN. Solid lines — dependences described by equations 3 (1, 2, 4) and 4 (3), accordingly.

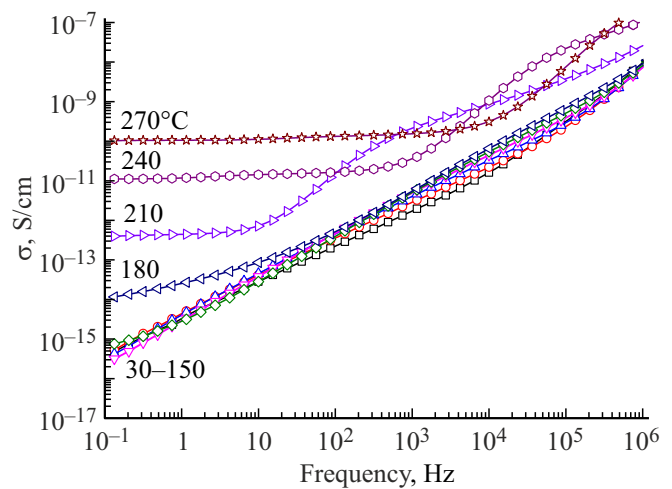


**Figure 7.** Frequency dependences  $\sigma_{ac}$  for nanocomposite film P-SOS + 3% CeO<sub>2</sub>

$\sigma_{ac} = \varphi(f)$  for nanocomposite P-SOS + 3% CeO<sub>2</sub> in the area of glassy and highly elastic state.

These dependences are typical for polymers [11,28,36]. At temperatures below vitrification temperature (figure does not include curves below 30°C) the dependences show linear growth of conductivity with frequency. In highly elastic state, dependences  $\sigma_{ac} = \varphi(f)$  demonstrate a fracture at frequency  $f_0$ , below which there is a plateau (no dependence on frequency). As temperature grows,  $f_0$  moves sequentially to high frequencies. Plateau on dependence  $\sigma_{ac} = \varphi(f)$  meets values  $\sigma_{dc}$ , which, actually, determine conductivity of the system in highly elastic state. At each temperature the area on the left from  $f_0$  meets the motion of charges to long distances, and in the area on the right — charges are spatially restricted in potential pits.

To compare values of conductivity for all studied systems, Table 4 includes values  $\sigma_{dc}$  at 270°C. It is seen that all values  $\sigma_{dc}$  are quite close, i.e. conductivity is not influenced a lot by chemical composition of the studied PI, but by introduction of nanoparticles CeO<sub>2</sub> in these matrices. Only in case of nanocomposite based on P-SOS one can say about certain reduction of conductivity (within limits of the same order) compared to initial PI.

In practical use of films of various PIs, the value of dielectric permeability is of great importance. It is determined using equation  $\epsilon' = C_s(14.4 \times d)/D^2$ , where  $C_s$  — capacity of the sample (dielectric cell), pF,  $d$  — thickness of the sample,  $\mu m$ , and  $D$  diameter of the upper electrode, cm. For all studied samples (both PIs and nanocomposites on their basis), values  $\epsilon'$  were within  $3.2 \pm 0.1$ .

#### 4. Molecular mechanisms of dielectric processes

When dielectric behavior of films of three poly nuclear PIs used in the paper were studied, as well as for the

**Table 4.** Values  $-\lg \tau_0$ ,  $B$ ,  $T_0$ ,  $T_g$  and  $\sigma_{dc}$  for films of studied PIs and nanocomposites

PI	$-\lg(\tau_0)$	$B, K$	$T_0, K$	$T_g, ^\circ C^*$	$\sigma_{dc}$ , at 270°C, S/cm
P-SOD	11.1	1426	440	222	165E-10
P-SOD+3% CeO <sub>2</sub>	10.6	1294	441	221	1.75E-10
P-SOS	11.4	1468	404	188	1.01E-10
P-SOS + 3% CeO <sub>2</sub>	12.0	1596	403	187	1.2E-11
P-OOD	10.4	1077	414	185.7	1.65E-10
P-OOD + 3% CeO <sub>2</sub>	12.6	1921	391	183.5	1.03E-10

Note.  $*T_g$  are defined at  $\lg \tau_{max} = 0$ .

previously studied polymers of this class,  $\alpha$ ,  $\beta$  and  $\gamma$  relaxation processes were found. In the spectra of all studied nanocomposites,  $\alpha$ ,  $\beta$  and  $\beta_1$  relaxation processes were observed (it was not possible to identify  $\gamma$  process). In papers [28–34,36–38], molecular mechanisms were proposed for  $\alpha$ ,  $\beta$  and  $\gamma$  processes. It is known that dielectric behavior of PIs is impacted by presence of moisture in the films and thermal prehistory [28,31,36,38]. To prevent influence of this factors at the results of the works performed, all studied film materials were exposed to preannealing at 300°C.

The molecular mechanism of  $\alpha$  process in PIs causes no doubts. It is related to disinhibition of large-scale segmental (cooperative) mobility of the main chain of the macromolecule and transition to highly elastic state [37–42].

Mechanisms for implementation of  $\gamma$  and  $\beta$  processes observed in glassy state are not identified so unambiguously. Comparison of dielectric properties of multiple PIs of various composition made it possible to relate the lowest temperature (the highest frequency)  $\gamma$  process with local non-cooperative mobility of connected water molecules, with limited fluctuations of phenylene rings in a diamine component of the macromolecule, or with reorientation of polar side groups in a dianhydride component [14–16,31,36,38]. Intensity of this process depends on thermal prehistory of the studied material, in particular — on the conditions of preliminary drying of the sample [15,32]. For some PIs preliminary thermal treatment of the film above 300°C fully suppresses  $\gamma$  process. For many PIs in the area of  $\gamma$  process temperature  $\lg \delta_{max}$  was weakly dependent on the composition of PIs and made  $\sim -100^\circ C$  (at 1 Hz). Temperature dependences of relaxation time of  $\gamma$  process comply with Arrhenius equation.  $E_a$  are relatively low ( $\sim 8-11$  kcal/mol), and value  $\tau_0 \sim 10^{-14}$  s, which meets the Debye process of non-cooperative type.  $\tau_0$  value is a parameter of size of the reoriented local group in the elementary unit: the lower the relaxation time, the smaller the group and the relaxation volume [43].

To identify mechanism of  $\beta$  relaxation, several hypotheses are proposed in literature sources. In paper [31] it is connected to mobility of dianhydride component of macromolecule. Authors of works [16,28,29,36] believed that  $\beta$  process was caused by rotation of paraphenylene sequences in a diamine component and/or sections of paraphenylene and imide groups in dianhydride component, accordingly.

For  $\beta$  process in PIs, wide distribution of relaxation times is specific, which is illustrative of contributions made to it by several elementary relaxation processes with close relaxation times. For some PIs, it was possible to identify two  $\beta$  processes [16,29,33]:  $\beta'$  and  $\beta''$ , provided for by reorientation of paraphenylene fragments in diamine part of macromolecule and reorientation of dianhydride fragments between imide cycles and imide cycles themselves, accordingly. Temperature dependences of relaxation time for  $\beta$  process comply with Arrhenius equation, parameters of which are sensitive to chemical structure of PIs with wide variation of the latter. Thus, values of activation energy are within the limits of 20–50 kcal/mol, and temperature of maximum  $\lg \delta$  at 1 Hz varies in the range of 50–150°C [29,31,33].

Analyzing the produced results, it is necessary to define the kinetic structural units included in the composition of units (such as polar groups), which may serve as the source of occurrence of relaxation processes in the studied systems in the glassy state. Based on the chemical structure, one can expect several mobility modes. In a diamine component of the macromolecule including four paraphenylene rings, connected by bridge groups, this may be a movement of one or two middle rings. In a dianhydride component such mobility modes may be reorientation of metaphenylene ring and imide groups.

It can be believed that the source of the fastest  $\gamma$  process for initial PIs is mobility of paraphenylene rings with adjacent polar groups  $-O-$ ,  $-SO_2-$  or  $-S-$ . Temperature of transition for  $\gamma$  process (position  $\epsilon''_{max}$  at 1 Hz) for P-SOD, P-SOS and P-OOD was  $-101$ ,  $-92$  and  $-96^\circ C$ , accordingly. Values of parameters of Arrhenius equation,  $E_a$  and  $\lg \tau_0$ , are typical for non-cooperative local type of molecular mobility and make  $\sim 11$  kcal/mol and  $\sim 13$  accordingly (Table 4), which is close to the values for the previously studied PI.

In the field of  $\beta$  process for P-SOD, P-SOS and P-OOD the values of parameters  $E_a$  and  $\lg \tau_0$  in Arrhenius equations are  $\sim 30$  kcal/mol and  $\sim 20$ , accordingly (Table 3). This suggests a certain contribution of intermolecular interactions and impact of heterogeneity of local environment and may be related to fluctuation of lengthier sections of the macromolecule. Such areas may be metaphenylene rings plus imide rings in a dianhydride component, as well as two-three para-phenylene rings with adjacent polar groups. Therefore, the source of  $\beta$  process is mobility of polar  $-O-$

and  $-\text{O}=\text{N}=\text{O}-$  (dianhydride fragment) and/or  $-\text{O}-$ ,  $-\text{SO}_2-$  or  $-\text{S}-$  groups (diamine fragment). Molecular mobility P-SOD, P-SOS and P-OOD for  $\beta$  process are weakly dependent on chemical structure; parameters of equation (3) are close, and temperatures  $\varepsilon''_{\max}$  (at 1 Hz) for P-SOD, P-SOS and P-OOD, are 81, 81 and 79°C accordingly, i.e. are within the limits of temperatures for previously studied PIs. This suggests that the process is an imposition of several molecular mobility modes with close relaxation times. This is confirmed by wide distribution of relaxation times ( $\alpha_{HN} = 0.25-0.35$ ). For these systems it was not possible to separate  $\beta$  process into two components,  $\beta'$  and  $\beta''$ .

Two features were observed for nanocomposites in glassy state: because of growing values of  $\text{tg } \delta$  and  $\varepsilon''$  it was not possible to identify  $\gamma$  process (Fig. 2), and in area of  $\beta$  process the dielectric spectra could be described by a sum of two HN processes (Fig. 4). For the first process the temperature-frequency position of dependence  $-\lg \tau_{\max} = \varphi(1/T)$  was close to such for  $\beta$  process in initial PIs (Table 3), and temperatures  $\varepsilon''_{\max}$  (at 1 Hz) make 81, 79 and 73°C accordingly. The second  $\beta_1$  process is observed at lower temperatures: relaxation times compared to  $\beta$  process is 1–4 orders lower (compare curves 3 and 4 in Fig. 5, b), and Arrhenius equation parameters are close to Debye non-cooperative process. Temperatures of transitions in  $\beta_1$  process for P-SOD + 3%  $\text{CeO}_2$ , P-SOS + 3%  $\text{CeO}_2$  and P-OOD + 3%  $\text{CeO}_2$  for  $\varepsilon''_{\max}$  at 1 Hz are 2,  $-5$  and  $-2$ °C accordingly. It is obvious that  $\beta_1$  process is caused by presence of nanoparticles in PI polymer matrix. For  $\beta$  and  $\beta_1$  process the molecular mobility practically does not depend on the chemical composition.

The highest temperature  $\alpha$  process, both in the case of initial PIs and for nanocomposites can be connected to large-scale segmental mobility of the main chain in the macromolecule. Temperature-frequency coordinates of  $\alpha$  process, dependences  $-\lg \tau_{\max} = \varphi(1/T)$ , separate the area of polymer glassy state (on the right) from highly elastic state (on the left). Vitrification temperatures of studied samples are defined by the procedure traditional for dielectric method — extrapolation of dependence  $-\lg \tau_{\max} = \varphi(1/T)$ , described by equation V–T–H, to  $\lg \tau_{\max} = 0$  ( $\tau_{\max} = 1$  s). Parameters of equation (4) are given in Table 4. For nanocomposites, temperature-frequency coordinates in the area of  $\alpha$  process are close to such for initial PIs. Accordingly, the vitrification temperature of each of studied PIs is practically identical to such for a nanocomposite formed on its basis (Table 4). This result fully complies with data produced by thermomechanical method (Table 2).

## 5. Conclusions

Research of dielectric behavior of films in some polynuclear PIs and composites on their basis filled with nanoscale

particles of cerium dioxide (3 mass.%), demonstrated several relaxation areas of dipole polarization:  $\gamma$  (only in initial PIs),  $\beta_1$  (only in nanocomposites),  $\beta$  and  $\alpha$  (in initial PIs and in nanocomposites) processes. Temperature dependences of relaxation time in areas  $\gamma$ ,  $\beta_1$  and  $\beta$  comply with Arrhenius equation, and in area of  $\alpha$  process are described by empirical equation V–T–H.

In areas of  $\gamma$  and  $\beta_1$  and  $\beta$  processes the molecular mobility is weakly dependent on the structure and complies with temperature-frequency coordinates of curve 1, 4 and 2 accordingly (Fig. 5). For  $\gamma$  and  $\beta_1$  and  $\beta$  processes the temperature  $\varepsilon''_{\max}$  at 1 Hz is near  $-100$ , 2 and 80°C accordingly. Molecular interpretation of each of these processes was given.

Introduction of cerium dioxide nanoparticles in PIs results in the fact that:

1. In glassy state, together with  $\beta$  process, a higher frequency (lower temperature)  $\beta_1$  process occurs;
2. Availability of  $\beta_1$  process is related specifically to presence of  $\text{Ce}_2\text{O}$  nanoparticles in the material and reflects interactions between them and polar groups of PI macromolecule, occurring when nanocomposite is formed.
3. Introduction of 3%  $\text{Ce}_2\text{O}$  into polymer causes no noticeable variation of segmental molecular mobility in area of  $\alpha$  process, since the intensity of this process, as well as relaxation times, are practically invariable compared to these characteristics of initial PIs.
4. Data on conductivity in highly elastic state demonstrates that for the studied film materials, values  $\sigma_{dc}$  vary slightly with variation of matrix PI structure and when cerium dioxide is introduced therein.

## Acknowledgments

Authors would like to express their gratitude to the staff of the High-Heat-Resistant Polymer Synthesis Laboratory, Institute of Macromolecular Compounds, Russian Academy of Sciences, who synthesized prepolymers for this paper.

## Funding

This study was carried out under financial support of the Russian Science Foundation (grant No. 22-13-00068).

## Conflict of interest

The authors declare that they have no conflict of interest.

## References

- [1] R.G. Bryant. Polyimides. In: Encyclopedia of polymer science and technology / Ed. H.F. Mark. 4th ed. John Wiley & Sons Publ., N.Y. (2002). V. 7. P. 529–555.
- [2] M.I. Bessonov, M.M. Koton, V.V. Kudryavtsev, L.A. Laius. Polyimides — Thermally Stable Polymers. Plenum Publishing Corp., N.Y. (1987). 318 p.
- [3] Y. Gogotsi. Nanomaterials handbook. Taylor and Francis, Boca Raton, London, N.Y. (2006). 779 p.

- [4] I. Zaman, B. Manshoor, A. Khalid, S. Araby. *J. Polymer Res.* **5**, 21, 429 (2014).
- [5] A. Kausar. *Polymer-Plast. Technol. Eng.* **56**, 13, 1375 (2017).
- [6] X. Wang, Q. Jiang, W. Xu, W. Cai, Y. Inoue, Y. Zhu. *Carbon* **53**, 145 (2013).
- [7] W.Y. Hsieh, K.B. Cheng, C.M. Wu. *J. Polymer Res.* **24**, 11, 205 (2017).
- [8] A.V. Eletskiy, A.A. Knizhnik, B.V. Potapkin, Kh.M. Kenni. *UFN* **58**, 3, 225 (2015) (in Russian)
- [9] V.E. Yudin, V.M. Svetlichnyi, A.N. Shumakov, R. Schechter, H. Harel, G. Marom. *Composites A* **39**, 1, 85 (2008).
- [10] I.V. Gofman, V.E. Yudin, O. Orell, J. Vuorinen, A.Ya. Grigoriev, V.M. Svetlichnyi. *J. Macromol. Sci. B* **52**, 12, 1848 (2013).
- [11] N.A. Nikonorova, A.A. Kononov, H.T. Dao, R.A. Castro. *J. Non-Cryst. Solids* **511**, 1, 109 (2019).
- [12] V.A. Gerasin, E.M. Antipov, V.V. Karbushev, V.G. Kulichikhin, G.P. Karpacheva, R.V. Talroze, Ya.V. Kudryavtsev. *Usp. khimii* **82**, 4, 303 (2013). (in Russian)
- [13] E.N. Bykova, I.V. Gofman, E.M. Ivan'kova, A.V. Yakimansky, O.S. Ivanova, A.E. Baranchikov, V.K. Ivanov. *Nanosystems: Phys. Chem., Math.* **10**, 6, 666 (2019).
- [14] J.D. Jacobs, M.J. Arlen, D.H. Wang, Z. Ounaies, R. Berry, L-S. Tan, P.H. Garret, R.A. Vaia. *Polymer* **51**, 14, 3139 (2010).
- [15] A.C. Comer, C.P. Ribeiro, B.D. Freeman, D.S. Kalika. *Polymer* **54**, 2, 891 (2013).
- [16] W. Qu, T-M. Ko, R.H. Vora, T-S. Cheng. *Polymer* **42**, 15, 6393 (2001).
- [17] J. van Turnhout, M. Wubbenhorst. *J. Non-Cryst. Solids* **305**, 1–3, 50 (2002).
- [18] Broadband dielectric spectroscopy / Eds F. Kremer, A. Schönhals. Springer, Berlin, Heidelberg (2012). 729 p.
- [19] E. Donth. *The glass transition: relaxation dynamics in liquids and disordered materials*. Springer, Berlin (2001). 448 p.
- [20] N.A. Nikonorova, M.Yu. Balakina, O.D. Fominykh, M.S. Pudovkin, T.A. Vakhonina, R. Diaz-Calleja, A.V. Yakimansky. *Chem. Phys. Lett.* **552**, 114 (2012).
- [21] I. Gofman, A. Nikolaeva, A. Yakimansky, O. Ivanova, A. Baranchikov, V. Ivanov. *Polymer Adv. Technol.* **30**, 6, 1518 (2019).
- [22] A. Nikolaeva, I. Gofman, A. Yakimansky, E. Ivan'kova, N. Gulii, M. Teplonogova, O. Ivanova, A. Baranchikov, V. Ivanov. *Mater. Today Commun.* **22**, 100803, (2020).
- [23] A.L. Nikolaeva, I.V. Gofman, A.V. Yakimansky, E.M. Ivan'kova, I.V. Abalov, A.E. Baranchikov, V.K. Ivanov. *Polymer* **12**, 9, 1952 (2020).
- [24] I.V. Gofman; I.V. Abalov, S.V. Gladchenko, N.V. Afanas'eva. *Polymer Adv. Technol.* **23**, 3, 408 (2012).
- [25] V.K. Ivanov, G.P. Kopitsa, A.E. Baranchikov, S.V. Grigor'ev, V.V. Runov, V.M. Haramus. *Russ. J. Inorg. Chem.* **54**, 12, 1857 (2009).
- [26] S. Havriliak, S. Negami. *Polymer* **8**, 161 (1967).
- [27] R. Diaz-Calleja. *Macromolecules* **33**, 24, 8924 (2000).
- [28] S. Chisca, V.E. Musteata, I.S.M. Bruma. *Eur. Polymer J.* **47**, 5, 1186 (2011).
- [29] Z. Sun, L. Dong, Y. Zhuang, L. Cao, M. Ding, Z. Feng. *Polymer* **33**, 22, 4728 (1992).
- [30] J.C. Coburn, P.D. Soper, B.C. Auman. *Macromolecules* **28**, 9, 3253 (1995).
- [31] S.Z.D. Cheng, T.M. Chalmes, Y. Gu, Y. Yoon, F.W. Harris, J. Cheng, M. Fone, J.L. Koenig. *Macromol. Chem. Phys.* **196**, 5, 1439 (1995).
- [32] G. Xu, C.C. Gryte, A.S. Nowick, S.Z. Li, Y.S. Pak, S.G. Greenbaum. *J. App. Phys.* **66**, 11, 5290 (1989).
- [33] H. Tang, L. Dong, M. Ding, Z. Feng. *Eur. Polymer J.* **32**, 10, 1221 (1996).
- [34] C. Bas, T. Pascal, N.D. Alberola. *Polymer Eng. Sci.* **43**, 2, 344 (2003).
- [35] A.M. Kamalov, M.E. Borisova, A.L. Didenko, N.A. Nikonorova, V.M. Svetlichnyi, V.E. Smirnova, R.A. Kastro, V.E. Yudin. *Polymer Sci. A.* **62**, 2, 107 (2020).
- [36] R. Khazaka, M.L. Locatelli, S. Diaham, P. Bidan, L. Dupuy, G. Grosset. *J. Phys. D* **46**, 6, 065501 (2013).
- [37] N.A. Nikonorova, A.L. Didenko, V.V. Kudryavtsev, R.A. Castro. *Non-Cryst. Solids* **447**, 117 (2016).
- [38] A.E. Eichstadt, S. Andreev, T.C. Ward. *Proc. Ann. Meeting Adhesion Soc.* **23**, 484 (2000).
- [39] J. Melchez, Y. Daben, G. Arlt. *IEEE Trans. Electr. Insul.* **24**, 1, 31 (1989).
- [40] M. Calle, C. Garcia. A.E. Lozano, J.G. de la Campa, J. de Abajo, C. Alvarez. *J. Membrane Sci.* **434**, 121 (2013).
- [41] P. Klonos, A. Panagopoulou, A. Kyritsis, L. Bokobza, P. Pissis. *J. Non-Cryst. Solids* **357**, 2, 610 (2011).
- [42] A. Fukam, K. Lisaka, S. Kubota, S. Etoh. *J. Appl. Polymer Sci.* **42**, 11, 3065 (1991).
- [43] C.J.F. Bottcher, P. Bordewijk. *Theory of electric polarization*. 2<sup>nd</sup> ed. Elsevier, Amsterdam (1978). V. 2, 377 p.